Supporting Information

Imaging Mass Spectrometry Reveals a Massive Loss of Polyunsaturated Cardiolipins in the Cortical Contusion, Hippocampus and Thalamus after Traumatic Brain Injury

L. J. Sparvero[1,2,*], A. A. Amoscato[1,2,*], A. B. Fink[1,2], T. Anthonymuthu[1], L.E. New[3], P.M. Kochanek[3], S. Watkins[4], V.E. Kagan,[1,2,#], and H. Bayır[1,2,3,#]

[1]Department of Environmental and Occupational Health, [2]Center for Free Radical and Antioxidant Health, [3]Department of Critical Care Medicine, and Safar Center for Resuscitation Research, [4]Department of Cell Biology, University of Pittsburgh, Pittsburgh, Pennsylvania

*These authors contributed equally to this work

[#]Corresponding authors for proofs and reprints:

Hülya Bayır, MD; bayihx@ccm.upmc.edu
Address: Children's Hospital of Pittsburgh.
4401 Penn Avenue
Pittsburgh, PA 15224

Valerian E. Kagan, PhD; kagan@pitt.edu
Address: Bridgeside Point
100 Technology Drive, Room 330
Pittsburgh, PA 15219-3130

Supplementary Figures. Tables, and Method

Supplementary Fig. 1: Statistically significant differences between ipsi-/contralateral ratios of different CL species in various CCI brain regions.

Supplementary Fig. 2: MALDI-MS images of the major ganglioside species from rat brain tissue.

Supplementary Fig. 3: Ratiometric images of CL in naïve rat brain tissue.

Supplementary Fig. 4: Ratiometric images of CL in CCI rat brain tissue.

Supplementary Table 1: CL species identified in rat brain based on MS/MS fragmentation as determined from LC-MS analysis.

Supplementary Table 2: Ipsilateral/contralateral intensity ratios for various lipids species.

Supporting Method 1: Spectra Acquisition and Data Conversion for .t2d Files on the ABI-4800 MALDI for Tissue Imaging with full random walking

Supplementary Figures

Figure 1: Tukey's post hoc test, CL species

(a) Contusional Cortex

	CL(74:7)	CL(76:11)	CL(74:9)	CL(74:8)	CL(76:10)	CL(74:6)	CL(76:12)	CL(72:5)	CL(72:7)	CL(74:10)	CL(72:6)	CL(76:9)	CL(72:4)	CL(72:8)	CL(72:9)	CL(74:11)	CL(70:5)	CL(70:7)	CL(70:4)	CL(70:6)	CL(72:3)	CL(76:8)	CL(70:3)
CL(74:7)		1.000	1.000	1.000	1.000	1.000	0.968	0.951	0.926	0.915	0.870	0.471	0.267	0.041	0.013	0.010	0.008	0.006	0.005	0.002	0.001	0.001	0.000
CL(76:11)	1.000		1.000	1.000	1.000	1.000	1.000	1.000	0.999	0.999	0.997	0.883	0.692	0.199	0.079	0.060	0.052	0.037	0.032	0.012	0.007	0.005	0.001
CL(74:9)	1.000	1.000		1.000	1.000	1.000	1.000	1.000	1.000	1.000	1.000	0.945	0.806	0.285	0.122	0.094	0.082	0.060	0.052	0.020	0.012	0.008	0.003
CL(74:8)	1.000	1.000	1.000		1.000	1.000	1.000	1.000	1.000	1.000	1.000	0.970	0.866	0.351	0.159	0.124	0.109	0.081	0.070	0.028	0.017	0.011	0.004
CL(76:10)	1.000	1.000	1.000	1.000		1.000	1.000	1.000	1.000	1.000	1.000	0.992	0.943	0.487	0.245	0.197	0.175	0.134	0.117	0.049	0.030	0.020	0.007
CL(74:6)	1.000	1.000	1.000	1.000	1.000		1.000	1.000	1.000	1.000	1.000	0.994	0.948	0.502	0.255	0.206	0.183	0.140	0.122	0.052	0.032	0.022	0.008
CL(76:12)	0.968	1.000	1.000	1.000	1.000	1.000		1.000	1.000	1.000	1.000	1.000	1.000	0.884	0.647	0.571	0.531	0.447	0.408	0.218	0.149	0.107	0.044
CL(72:5)	0.951	1.000	1.000	1.000	1.000	1.000	1.000		1.000	1.000	1.000	1.000	1.000	0.915	0.702	0.628	0.588	0.502	0.462	0.256	0.177	0.130	0.054
CL(72:7)	0.926	0.999	1.000	1.000	1.000	1.000	1.000	1.000		1.000	1.000	1.000	1.000	0.943	0.760	0.690	0.651	0.565	0.524	0.303	0.214	0.158	0.068
CL(74:10)	0.915	0.999	1.000	1.000	1.000	1.000	1.000	1.000	1.000		1.000	1.000	1.000	0.951	0.779	0.711	0.673	0.587	0.546	0.320	0.228	0.169	0.074
CL(72:6)	0.870	0.997	1.000	1.000	1.000	1.000	1.000	1.000	1.000	1.000		1.000	1.000	0.973	0.842	0.782	0.747	0.666	0.625	0.388	0.283	0.215	0.097
CL(76:9)	0.471	0.883	0.945	0.970	0.992	0.994	1.000	1.000	1.000	1.000	1.000		1.000	1.000	0.994	0.986	0.981	0.961	0.947	0.806	0.693	0.594	0.355
CL(72:4)	0.267	0.692	0.806	0.866	0.943	0.948	1.000	1.000	1.000	1.000	1.000	1.000		1.000	1.000	0.999	0.999	0.996	0.993	0.945	0.884	0.814	0.581
CL(72:8)	0.041	0.199	0.285	0.351	0.487	0.502	0.884	0.915	0.943	0.951	0.973	1.000	1.000		1.000	1.000	1.000	1.000	1.000	1.000	1.000	0.998	0.971
CL(72:9)	0.013	0.079	0.122	0.159	0.245	0.255	0.647	0.702	0.760	0.779	0.842	0.994	1.000	1.000		1.000	1.000	1.000	1.000	1.000	1.000	1.000	0.999
CL(74:11)	0.010	0.060	0.094	0.124	0.197	0.206	0.571	0.628	0.690	0.711	0.782	0.986	0.999	1.000	1.000		1.000	1.000	1.000	1.000	1.000	1.000	1.000
CL(70:5)	0.008	0.052	0.082	0.109	0.175	0.183	0.531	0.588	0.651	0.673	0.747	0.981	0.999	1.000	1.000	1.000		1.000	1.000	1.000	1.000	1.000	1.000
CL(70:7)	0.006	0.037	0.060	0.081	0.134	0.140	0.447	0.502	0.565	0.587	0.666	0.961	0.996	1.000	1.000	1.000	1.000		1.000	1.000	1.000	1.000	1.000
CL(70:4)	0.005	0.032	0.052	0.070	0.117	0.122	0.408	0.462	0.524	0.546	0.625	0.947	0.993	1.000	1.000	1.000	1.000	1.000		1.000	1.000	1.000	1.000
CL(70:6)	0.002	0.012	0.020	0.028	0.049	0.052	0.218	0.256	0.303	0.320	0.388	0.806	0.945	1.000	1.000	1.000	1.000	1.000	1.000		1.000	1.000	1.000
CL(72:3)	0.001	0.007	0.012	0.017	0.030	0.032	0.149	0.177	0.214	0.228	0.283	0.693	0.884	1.000	1.000	1.000	1.000	1.000	1.000	1.000		1.000	1.000
CL(76:8)	0.001	0.005	0.008	0.011	0.020	0.022	0.107	0.130	0.158	0.169	0.215	0.594	0.814	0.998	1.000	1.000	1.000	1.000	1.000	1.000	1.000		1.000
CL(70:3)	0.000	0.001	0.003	0.004	0.007	0.008	0.044	0.054	0.068	0.074	0.097	0.355	0.581	0.971	0.999	1.000	1.000	1.000	1.000	1.000	1.000	1.000	

(b) Non-contusional Cortex

	CL(76:8)	CL(72:3)	CL(76:11)	CL(76:9)	CL(70:7)	CL(74:11)	CL(72:9)	CL(70:5)	CL(70:3)	CL(74:10)	CL(70:6)	CL(76:12)	CL(76:10)	CL(70:4)	CL(74:9)	CL(74:8)	CL(72:4)	CL(72:7)	CL(72:6)	CL(74:6)	CL(72:5)	CL(74:7)	CL(72:8)
CL(76:8)		1.000	1.000	1.000	1.000	1.000	1.000	1.000	1.000	1.000	1.000	1.000	1.000	1.000	1.000	1.000	1.000	1.000	1.000	0.998	0.985	0.927	0.769
CL(72:3)	1.000		1.000	1.000	1.000	1.000	1.000	1.000	1.000	1.000	1.000	1.000	1.000	1.000	1.000	1.000	1.000	1.000	1.000	0.999	0.990	0.942	0.798
CL(76:11)	1.000	1.000		1.000	1.000	1.000	1.000	1.000	1.000	1.000	1.000	1.000	1.000	1.000	1.000	1.000	1.000	1.000	1.000	1.000	0.996	0.971	0.867
CL(76:9)	1.000	1.000	1.000		1.000	1.000	1.000	1.000	1.000	1.000	1.000	1.000	1.000	1.000	1.000	1.000	1.000	1.000	1.000	1.000	0.999	0.985	0.914
CL(70:7)	1.000	1.000	1.000	1.000		1.000	1.000	1.000	1.000	1.000	1.000	1.000	1.000	1.000	1.000	1.000	1.000	1.000	1.000	1.000	0.999	0.990	0.933
CL(74:11)	1.000	1.000	1.000	1.000	1.000		1.000	1.000	1.000	1.000	1.000	1.000	1.000	1.000	1.000	1.000	1.000	1.000	1.000	1.000	1.000	0.994	0.949
CL(72:9)	1.000	1.000	1.000	1.000	1.000	1.000		1.000	1.000	1.000	1.000	1.000	1.000	1.000	1.000	1.000	1.000	1.000	1.000	1.000	1.000	0.994	0.950
CL(70:5)	1.000	1.000	1.000	1.000	1.000	1.000	1.000		1.000	1.000	1.000	1.000	1.000	1.000	1.000	1.000	1.000	1.000	1.000	1.000	1.000	0.997	0.965
CL(70:3)	1.000	1.000	1.000	1.000	1.000	1.000	1.000	1.000		1.000	1.000	1.000	1.000	1.000	1.000	1.000	1.000	1.000	1.000	1.000	1.000	0.997	0.970
CL(74:10)	1.000	1.000	1.000	1.000	1.000	1.000	1.000	1.000	1.000		1.000	1.000	1.000	1.000	1.000	1.000	1.000	1.000	1.000	1.000	1.000	0.997	0.971
CL(70:6)	1.000	1.000	1.000	1.000	1.000	1.000	1.000	1.000	1.000	1.000		1.000	1.000	1.000	1.000	1.000	1.000	1.000	1.000	1.000	1.000	0.998	0.977
CL(76:12)	1.000	1.000	1.000	1.000	1.000	1.000	1.000	1.000	1.000	1.000	1.000		1.000	1.000	1.000	1.000	1.000	1.000	1.000	1.000	1.000	0.998	0.977
CL(76:10)	1.000	1.000	1.000	1.000	1.000	1.000	1.000	1.000	1.000	1.000	1.000	1.000		1.000	1.000	1.000	1.000	1.000	1.000	1.000	1.000	0.999	0.986
CL(70:4)	1.000	1.000	1.000	1.000	1.000	1.000	1.000	1.000	1.000	1.000	1.000	1.000	1.000		1.000	1.000	1.000	1.000	1.000	1.000	1.000	0.999	0.989
CL(74:9)	1.000	1.000	1.000	1.000	1.000	1.000	1.000	1.000	1.000	1.000	1.000	1.000	1.000	1.000		1.000	1.000	1.000	1.000	1.000	1.000	1.000	0.998
CL(74:8)	1.000	1.000	1.000	1.000	1.000	1.000	1.000	1.000	1.000	1.000	1.000	1.000	1.000	1.000	1.000		1.000	1.000	1.000	1.000	1.000	1.000	0.998
CL(72:4)	1.000	1.000	1.000	1.000	1.000	1.000	1.000	1.000	1.000	1.000	1.000	1.000	1.000	1.000	1.000	1.000		1.000	1.000	1.000	1.000	1.000	1.000
CL(72:7)	1.000	1.000	1.000	1.000	1.000	1.000	1.000	1.000	1.000	1.000	1.000	1.000	1.000	1.000	1.000	1.000	1.000		1.000	1.000	1.000	1.000	1.000
CL(72:6)	1.000	1.000	1.000	1.000	1.000	1.000	1.000	1.000	1.000	1.000	1.000	1.000	1.000	1.000	1.000	1.000	1.000	1.000		1.000	1.000	1.000	1.000
CL(74:6)	0.998	0.999	1.000	1.000	1.000	1.000	1.000	1.000	1.000	1.000	1.000	1.000	1.000	1.000	1.000	1.000	1.000	1.000	1.000		1.000	1.000	1.000
CL(72:5)	0.985	0.990	0.996	0.999	0.999	1.000	1.000	1.000	1.000	1.000	1.000	1.000	1.000	1.000	1.000	1.000	1.000	1.000	1.000	1.000		1.000	1.000
CL(74:7)	0.927	0.942	0.971	0.985	0.990	0.994	0.994	0.997	0.997	0.997	0.998	0.998	0.999	0.999	1.000	1.000	1.000	1.000	1.000	1.000	1.000		1.000
CL(72:8)	0.769	0.798	0.867	0.914	0.933	0.949	0.950	0.965	0.970	0.971	0.977	0.977	0.986	0.989	0.998	0.998	1.000	1.000	1.000	1.000	1.000	1.000	

(c) Hippocampus

	CL(74:7)	CL(76:11)	CL(74:8)	CL(76:10)	CL(74:9)	CL(74:6)	CL(76:9)	CL(72:7)	CL(72:5)	CL(72:6)	CL(76:12)	CL(72:4)	CL(74:10)	CL(70:4)	CL(76:8)	CL(70:5)	CL(70:3)	CL(72:3)	CL(70:6)	CL(70:7)	CL(72:8)	CL(72:9)	CL(74:11)
CL(74:7)		1.000	0.999	0.987	0.983	0.935	0.388	0.297	0.167	0.105	0.041	0.019	0.015	0.000	0.000	0.000	0.000	0.000	0.000	0.000	0.000	0.000	0.000
CL(76:11)	1.000		1.000	1.000	1.000	1.000	0.946	0.896	0.744	0.606	0.358	0.212	0.175	0.001	0.001	0.001	0.000	0.000	0.000	0.000	0.000	0.000	0.000
CL(74:8)	0.999	1.000		1.000	1.000	1.000	0.992	0.978	0.908	0.814	0.573	0.384	0.327	0.003	0.002	0.002	0.001	0.001	0.000	0.000	0.000	0.000	0.000
CL(76:10)	0.987	1.000	1.000		1.000	1.000	1.000	0.999	0.986	0.954	0.807	0.628	0.562	0.008	0.008	0.007	0.003	0.003	0.001	0.001	0.001	0.000	0.000
CL(74:9)	0.983	1.000	1.000	1.000		1.000	1.000	0.999	0.990	0.963	0.832	0.660	0.595	0.009	0.009	0.008	0.004	0.003	0.001	0.001	0.001	0.000	0.000
CL(74:6)	0.935	1.000	1.000	1.000	1.000		1.000	1.000	0.999	0.993	0.935	0.817	0.762	0.019	0.018	0.017	0.008	0.006	0.003	0.003	0.002	0.000	0.000
CL(76:9)	0.388	0.946	0.992	1.000	1.000	1.000		1.000	1.000	1.000	1.000	0.999	0.998	0.197	0.186	0.180	0.100	0.082	0.045	0.040	0.025	0.004	0.000
CL(72:7)	0.297	0.896	0.978	0.999	0.999	1.000	1.000		1.000	1.000	1.000	1.000	1.000	0.268	0.254	0.247	0.143	0.119	0.067	0.059	0.038	0.007	0.000
CL(72:5)	0.167	0.744	0.908	0.986	0.990	0.999	1.000	1.000		1.000	1.000	1.000	1.000	0.439	0.421	0.411	0.261	0.223	0.135	0.120	0.080	0.016	0.001
CL(72:6)	0.105	0.606	0.814	0.954	0.963	0.993	1.000	1.000	1.000		1.000	1.000	1.000	0.580	0.561	0.550	0.375	0.327	0.209	0.189	0.129	0.029	0.001
CL(76:12)	0.041	0.358	0.573	0.807	0.832	0.935	1.000	1.000	1.000	1.000		1.000	1.000	0.820	0.804	0.796	0.627	0.570	0.410	0.378	0.278	0.076	0.004
CL(72:4)	0.019	0.212	0.384	0.628	0.660	0.817	0.999	1.000	1.000	1.000	1.000		1.000	0.936	0.928	0.923	0.806	0.758	0.601	0.566	0.446	0.146	0.009
CL(74:10)	0.015	0.175	0.327	0.562	0.595	0.762	0.998	1.000	1.000	1.000	1.000	1.000		0.959	0.953	0.950	0.855	0.814	0.667	0.632	0.510	0.179	0.011
CL(70:4)	0.000	0.001	0.003	0.008	0.009	0.019	0.197	0.268	0.439	0.580	0.820	0.936	0.959		1.000	1.000	1.000	1.000	1.000	1.000	1.000	0.998	0.641
CL(76:8)	0.000	0.001	0.002	0.008	0.009	0.018	0.186	0.254	0.421	0.561	0.804	0.928	0.953	1.000		1.000	1.000	1.000	1.000	1.000	1.000	0.998	0.660
CL(70:5)	0.000	0.001	0.002	0.007	0.008	0.017	0.180	0.247	0.411	0.550	0.796	0.923	0.950	1.000	1.000		1.000	1.000	1.000	1.000	1.000	0.998	0.670
CL(70:3)	0.000	0.000	0.001	0.003	0.004	0.008	0.100	0.143	0.261	0.375	0.627	0.806	0.855	1.000	1.000	1.000		1.000	1.000	1.000	1.000	1.000	0.830
CL(72:3)	0.000	0.000	0.001	0.003	0.003	0.006	0.082	0.119	0.223	0.327	0.570	0.758	0.814	1.000	1.000	1.000	1.000		1.000	1.000	1.000	1.000	0.870
CL(70:6)	0.000	0.000	0.000	0.001	0.001	0.003	0.045	0.067	0.135	0.209	0.410	0.601	0.667	1.000	1.000	1.000	1.000	1.000		1.000	1.000	1.000	0.951
CL(70:7)	0.000	0.000	0.000	0.001	0.001	0.003	0.040	0.059	0.120	0.189	0.378	0.566	0.632	1.000	1.000	1.000	1.000	1.000	1.000		1.000	1.000	0.962
CL(72:8)	0.000	0.000	0.000	0.001	0.001	0.002	0.025	0.038	0.080	0.129	0.278	0.446	0.510	1.000	1.000	1.000	1.000	1.000	1.000	1.000		1.000	0.986
CL(72:9)	0.000	0.000	0.000	0.000	0.000	0.000	0.004	0.007	0.016	0.029	0.076	0.146	0.179	0.998	0.998	0.998	1.000	1.000	1.000	1.000	1.000		1.000
CL(74:11)	0.000	0.000	0.000	0.000	0.000	0.000	0.000	0.000	0.001	0.001	0.004	0.009	0.011	0.641	0.660	0.670	0.830	0.870	0.951	0.962	0.986	1.000	

(d) Thalamus

	CL(76:11)	CL(76:10)	CL(74:8)	CL(76:12)	CL(74:10)	CL(74:9)	CL(74:7)	CL(76:9)	CL(72:6)	CL(72:7)	CL(72:5)	CL(72:8)	CL(72:4)	CL(74:6)	CL(70:3)	CL(70:4)	CL(74:11)	CL(76:8)	CL(70:6)	CL(72:9)	CL(70:5)	CL(72:3)	CL(70:7)
CL(76:11)		1.000	1.000	1.000	1.000	0.996	0.908	0.885	0.543	0.281	0.269	0.223	0.137	0.075	0.058	0.051	0.043	0.028	0.021	0.016	0.013	0.001	0.001
CL(76:10)	1.000		1.000	1.000	1.000	1.000	0.986	0.979	0.782	0.502	0.485	0.421	0.286	0.171	0.137	0.122	0.105	0.072	0.055	0.044	0.037	0.004	0.002
CL(74:8)	1.000	1.000		1.000	1.000	1.000	1.000	1.000	0.963	0.805	0.792	0.733	0.577	0.404	0.342	0.311	0.276	0.204	0.163	0.135	0.115	0.016	0.009
CL(76:12)	1.000	1.000	1.000		1.000	1.000	1.000	1.000	0.987	0.890	0.880	0.835	0.697	0.520	0.451	0.416	0.375	0.286	0.233	0.197	0.170	0.026	0.015
CL(74:10)	1.000	1.000	1.000	1.000		1.000	1.000	1.000	0.993	0.926	0.918	0.882	0.761	0.590	0.519	0.482	0.439	0.342	0.282	0.240	0.210	0.034	0.021
CL(74:9)	0.996	1.000	1.000	1.000	1.000		1.000	1.000	1.000	0.994	0.993	0.986	0.948	0.855	0.802	0.771	0.730	0.626	0.551	0.492	0.446	0.101	0.064
CL(74:7)	0.908	0.986	1.000	1.000	1.000	1.000		1.000	1.000	1.000	1.000	1.000	0.999	0.989	0.978	0.970	0.958	0.914	0.872	0.831	0.793	0.300	0.211
CL(76:9)	0.885	0.979	1.000	1.000	1.000	1.000	1.000		1.000	1.000	1.000	1.000	0.999	0.993	0.985	0.979	0.969	0.933	0.897	0.860	0.826	0.333	0.238
CL(72:6)	0.543	0.782	0.963	0.987	0.993	1.000	1.000	1.000		1.000	1.000	1.000	1.000	1.000	1.000	1.000	1.000	0.998	0.996	0.992	0.987	0.708	0.582
CL(72:7)	0.281	0.502	0.805	0.890	0.926	0.994	1.000	1.000	1.000		1.000	1.000	1.000	1.000	1.000	1.000	1.000	1.000	1.000	1.000	1.000	0.921	0.845
CL(72:5)	0.269	0.485	0.792	0.880	0.918	0.993	1.000	1.000	1.000	1.000		1.000	1.000	1.000	1.000	1.000	1.000	1.000	1.000	1.000	1.000	0.929	0.856
CL(72:8)	0.223	0.421	0.733	0.835	0.882	0.986	1.000	1.000	1.000	1.000	1.000		1.000	1.000	1.000	1.000	1.000	1.000	1.000	1.000	1.000	0.954	0.898
CL(72:4)	0.137	0.286	0.577	0.697	0.761	0.948	0.999	0.999	1.000	1.000	1.000	1.000		1.000	1.000	1.000	1.000	1.000	1.000	1.000	1.000	0.988	0.964
CL(74:6)	0.075	0.171	0.404	0.520	0.590	0.855	0.989	0.993	1.000	1.000	1.000	1.000	1.000		1.000	1.000	1.000	1.000	1.000	1.000	1.000	0.999	0.993
CL(70:3)	0.058	0.137	0.342	0.451	0.519	0.802	0.978	0.985	1.000	1.000	1.000	1.000	1.000	1.000		1.000	1.000	1.000	1.000	1.000	1.000	0.999	0.997
CL(70:4)	0.051	0.122	0.311	0.416	0.482	0.771	0.970	0.979	1.000	1.000	1.000	1.000	1.000	1.000	1.000		1.000	1.000	1.000	1.000	1.000	1.000	0.998
CL(74:11)	0.043	0.105	0.276	0.375	0.439	0.730	0.958	0.969	1.000	1.000	1.000	1.000	1.000	1.000	1.000	1.000		1.000	1.000	1.000	1.000	1.000	0.999
CL(76:8)	0.028	0.072	0.204	0.286	0.342	0.626	0.914	0.933	0.998	1.000	1.000	1.000	1.000	1.000	1.000	1.000	1.000		1.000	1.000	1.000	1.000	1.000
CL(70:6)	0.021	0.055	0.163	0.233	0.282	0.551	0.872	0.897	0.996	1.000	1.000	1.000	1.000	1.000	1.000	1.000	1.000	1.000		1.000	1.000	1.000	1.000
CL(72:9)	0.016	0.044	0.135	0.197	0.240	0.492	0.831	0.860	0.992	1.000	1.000	1.000	1.000	1.000	1.000	1.000	1.000	1.000	1.000		1.000	1.000	1.000
CL(70:5)	0.013	0.037	0.115	0.170	0.210	0.446	0.793	0.826	0.987	1.000	1.000	1.000	1.000	1.000	1.000	1.000	1.000	1.000	1.000	1.000		1.000	1.000
CL(72:3)	0.001	0.004	0.016	0.026	0.034	0.101	0.300	0.333	0.708	0.921	0.929	0.954	0.988	0.999	0.999	1.000	1.000	1.000	1.000	1.000	1.000		1.000
CL(70:7)	0.001	0.002	0.009	0.015	0.021	0.064	0.211	0.238	0.582	0.845	0.856	0.898	0.964	0.993	0.997	0.998	0.999	1.000	1.000	1.000	1.000	1.000	

Fig. 1: Statistically significant differences between ipsi-/contralateral ratios of different CL species in various CCI brain regions. Tukey's post hoc test was performed by treating the ipsi-/contralateral ratios of each CL species as a group within each of the following regions: the contusional cortex (a), an adjacent non-contusional cortical area (b), the hippocampus (c) and thalamus (d). CL species are arranged within the tables in the same order as described in Figure 3 (i.e. the CL species exhibiting the most loss ipsi-/contralaterally on the left/top and proceeding to those that lost the least on the right/bottom). The cells give the p-value between two CL species, and p-values < 0.050 are highlighted in red. For example, in the contusional cortex (a) the ipsi-/contralateral ratios of CL(74:7) are not significantly different from those of CL(76:11) but are significantly different from CL(70:3).

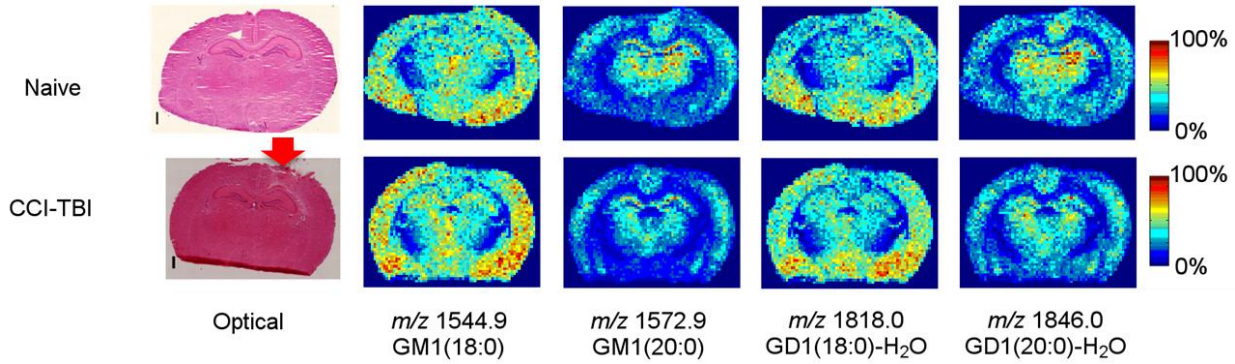

Fig. 2: MALDI-MS images of the major ganglioside species from rat brain tissue. IMS negative ion mode heat maps of the major PI and sulfatide species in naïve and CCI-TBI rat brain tissue sections treated with EDC-PLC (representative images from 3 animals). A corresponding H&E optical image (scale bar = 1 mm) is shown for both naïve and CCI-TBI tissue. Ganglioside species include GM1 (18:0), *m/z* 1544.9; GM1 (20:0), *m/z* 1572.9; GD1 (18:0)-H_2O, *m/z* 1818.0 and GD1 (20:0)-H_2O, *m/z* 1846.0. Arrow indicates the point of impact on the CCI tissue. MALDI-MS images are displayed as relative intensities.

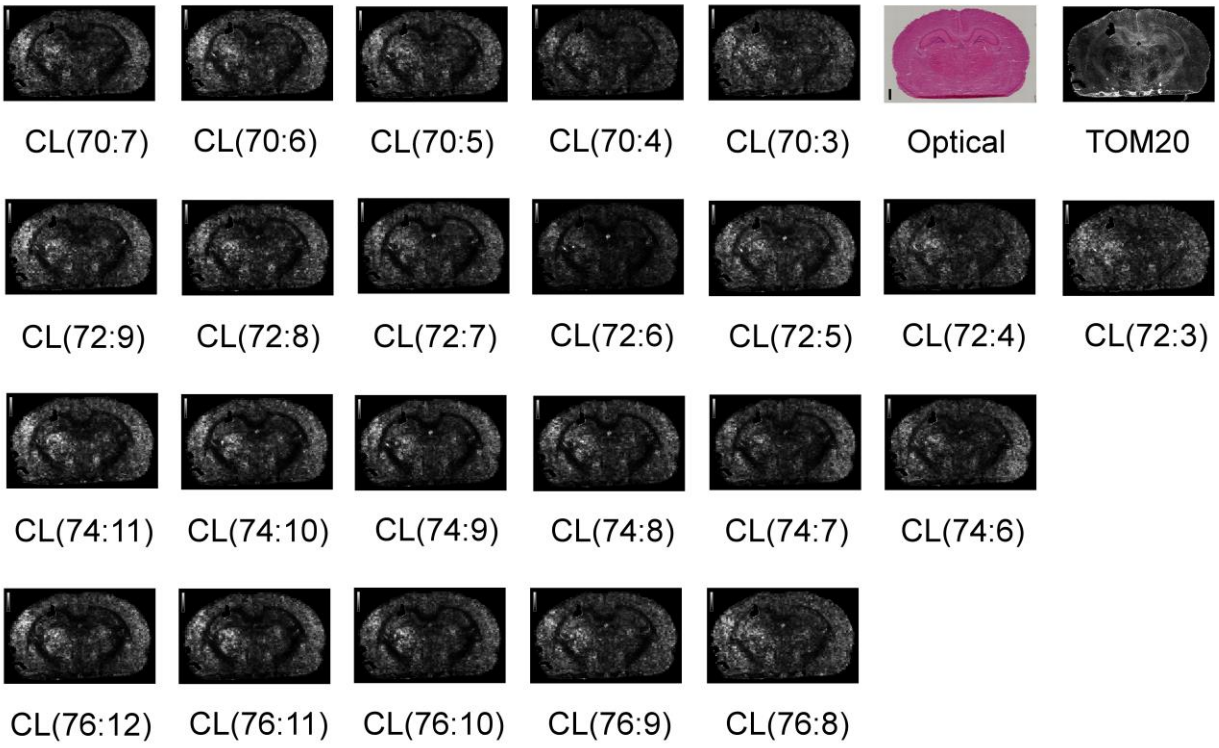

Fig. 3: Ratiometric images of CL in naïve rat brain tissue.

Ratiometric analysis of CL-IMS intensity to mitochondrial immunofluorescence intensity was assessed. Rat brain coronal sections (right hemispheres) were prepared for CL-IMS and CL heat maps were generated. Semi-serial brain sections were also prepared for mitochondrial immunohistochemical (IHC) staining using a fluorescent-labeled TOM 20 antibody. Ratiometric images for individual CL species are presented. MS image intensities for 23 individual CL species were rendered to a 12 bit range and ratioed with the mitochondrial IHC image and displayed as monochrome heat maps on a scale from 0 (black, less CL relative to mitochondria) to 50 (white, more CL relative to mitochondria). Ratiometric images of CL from clusters 70:X, 72:X , 74:X and 76:X are presented. In addition, an optical IHC H&E image (scale bar = 1 mm) and a TOM 20 IHC image are also shown.

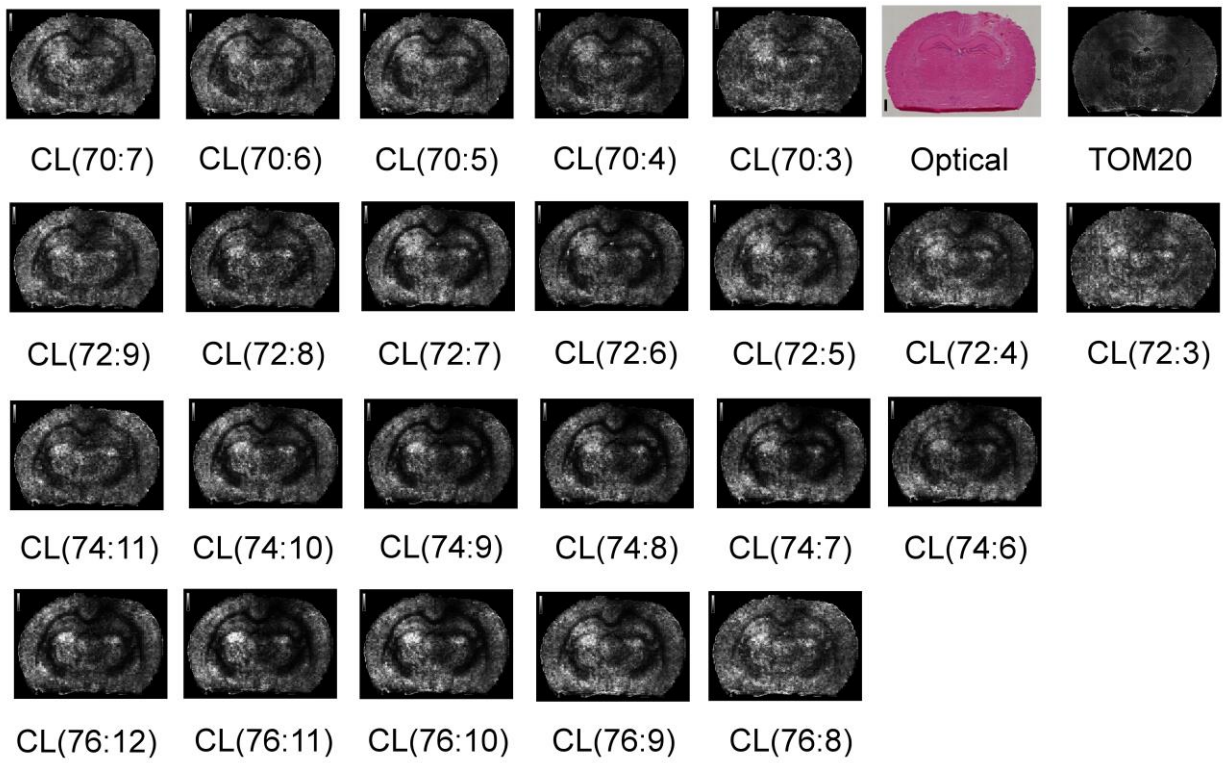

Fig. 4: Ratiometric images of CL in CCI rat brain tissue.
Ratiometric analysis of CL-IMS intensity to mitochondrial immunofluorescence intensity was assessed. CCI rat brain coronal sections were prepared for CL-IMS and CL heat maps were generated. Semi-serial brain sections were also prepared for mitochondrial immunohistochemical (IHC) staining using a fluorescent-labeled TOM 20 antibody. Ratiometric images for individual CL species are presented. MS image intensities for 23 individual CL species were rendered to a 12 bit range and ratioed with the mitochondrial IHC image and displayed as monochrome heat maps on a scale from 0 (black, less CL relative to mitochondria) to 50 (white, more CL relative to mitochondria). Ratiometric images of CL from clusters 70:X, 72:X , 74:X and 76:X are presented. In addition, an optical IHC H&E image (scale bar = 1 mm) and a TOM 20 IHC image are also shown.

Supplementary Tables

Table 1: CL species identified in rat brain based on MS/MS fragmentation as determined from LC-MS analysis.

Acyl Carbons: Double bonds	No PUFA	One PUFA	Two PUFA	Three PUFA	Four PUFA
70:10		$C_{16:1}C_{16:2}C_{18:1}C_{20:6}$	$C_{16:1}C_{16:1}C_{18:2}C_{20:6}$		$C_{16:2}C_{16:2}C_{18:2}C_{20:4}$
70:8		$C_{14:0}C_{16:1}C_{18:1}C_{22:6}$	$C_{14:0}C_{16:0}C_{18:2}C_{22:6}$	$C_{14:0}C_{18:2}C_{18:2}C_{20:4}$	
		$C_{16:0}C_{16:1}C_{16:1}C_{22:6}$	$C_{14:0}C_{16:0}C_{20:4}C_{20:4}$		
			$C_{16:1}C_{16:1}C_{18:2}C_{20:4}$		
70:7		$C_{16:1}C_{16:1}C_{18:1}C_{20:4}$	$C_{14:0}C_{18:1}C_{18:2}C_{20:4}$	$C_{16:1}C_{18:2}C_{18:2}C_{18:2}$	
			$C_{16:0}C_{16:1}C_{18:2}C_{20:4}$		
70:6		$C_{16:0}C_{16:1}C_{18:1}C_{20:4}$	$C_{16:1}C_{18:1}C_{18:2}C_{18:2}$	$C_{16:0}C_{18:2}C_{18:2}C_{18:2}$	
		$C_{14:0}C_{18:1}C_{18:1}C_{20:4}$	$C_{16:0}C_{16:0}C_{18:2}C_{20:4}$		
70:5	$C_{16:1}C_{16:1}C_{18:2}C_{20:1}$	$C_{16:0}C_{16:1}C_{18:1}C_{20:3}$	$C_{16:0}C_{16:0}C_{18:2}C_{20:3}$		
		$C_{16:1}C_{18:1}C_{18:1}C_{18:2}$	$C_{16:0}C_{18:1}C_{18:2}C_{18:2}$		
		$C_{14:0}C_{16:1}C_{20:3}C_{20:1}$	$C_{14:0}C_{18:2}C_{18:2}C_{20:1}$		
		$C_{16:0}C_{16:0}C_{18:1}C_{20:4}$			
		$C_{14:0}C_{16:0}C_{20:4}C_{20:1}$			
		$C_{14:0}C_{18:1}C_{18:1}C_{20:3}$			
70:4	$C_{16:1}C_{18:1}C_{18:1}C_{18:1}$	$C_{16:1}C_{18:0}C_{18:1}C_{18:2}$	$C_{16:0}C_{18:0}C_{18:2}C_{18:2}$		
		$C_{16:0}C_{18:1}C_{18:1}C_{18:2}$			
		$C_{14:0}C_{18:0}C_{18:0}C_{20:4}$			
		$C_{16:0}C_{16:0}C_{18:0}C_{20:4}$			
70:3	$C_{16:0}C_{18:1}C_{18:1}C_{18:1}$				
70:2	$C_{16:1}C_{18:0}C_{18:0}C_{18:1}$				
	$C_{16:0}C_{18:0}C_{18:1}C_{18:1}$				
72:10			$C_{16:1}C_{16:1}C_{18:2}C_{22:6}$		
			$C_{16:1}C_{16:1}C_{20:4}C_{20:4}$		
72:9		$C_{16:1}C_{16:1}C_{18:1}C_{22:6}$	$C_{14:0}C_{16:0}C_{20:3}C_{22:6}$		
			$C_{14:0}C_{18:1}C_{18:2}C_{22:6}$	$C_{14:0}C_{18:2}C_{20:4}C_{20:3}$	
			$C_{14:0}C_{18:1}C_{20:4}C_{20:4}$	$C_{16:1}C_{18:2}C_{18:2}C_{20:4}$	
			$C_{16:1}C_{16:1}C_{20:4}C_{20:3}$		
			$C_{16:0}C_{16:1}C_{18:2}C_{22:6}$		
			$C_{16:0}C_{16:1}C_{20:4}C_{20:4}$		
72:8		$C_{16:0}C_{16:1}C_{18:1}C_{22:6}$	$C_{16:1}C_{18:1}C_{18:2}C_{20:4}$	$C_{16:0}C_{18:2}C_{18:2}C_{20:4}$	$C_{18:2}C_{18:2}C_{18:2}C_{18:2}$
		$C_{14:0}C_{18:1}C_{18:1}C_{22:6}$	$C_{16:0}C_{16:0}C_{18:2}C_{22:6}$		
			$C_{16:0}C_{16:0}C_{20:4}C_{20:4}$		
72:7		$C_{16:1}C_{18:1}C_{18:1}C_{20:4}$	$C_{16:0}C_{16:1}C_{20:3}C_{20:3}$	$C_{16:0}C_{18:2}C_{18:2}C_{20:3}$	

			$C_{16:1}C_{18:1}C_{18:2}C_{20:3}$	$C_{18:1}C_{18:2}C_{18:2}C_{18:2}$	
			$C_{16:1}C_{18:0}C_{18:2}C_{20:4}$		
			$C_{16:0}C_{16:0}C_{20:4}C_{20:3}$		
			$C_{16:0}C_{18:1}C_{18:2}C_{20:4}$		
			$C_{14:0}C_{18:1}C_{20:3}C_{20:3}$		
			$C_{14:0}C_{18:0}C_{20:4}C_{20:3}$		
72:6		$C_{16:1}C_{18:1}C_{18:1}C_{20:3}$	$C_{16:1}C_{18:0}C_{18:2}C_{20:3}$	$C_{18:0}C_{18:2}C_{18:2}C_{18:2}$	
		$C_{16:1}C_{18:0}C_{18:1}C_{20:4}$	$C_{18:1}C_{18:1}C_{18:2}C_{18:2}$		
		$C_{16:0}C_{18:1}C_{18:1}C_{20:4}$	$C_{16:0}C_{18:1}C_{18:2}C_{20:3}$		
			$C_{16:0}C_{18:0}C_{18:2}C_{20:4}$		
			$C_{16:0}C_{16:0}C_{20:3}C_{20:3}$		
72:5		$C_{16:1}C_{18:0}C_{18:0}C_{20:4}$	$C_{18:0}C_{18:1}C_{18:2}C_{18:2}$		
		$C_{18:1}C_{18:1}C_{18:1}C_{18:2}$			
		$C_{16:0}C_{18:0}C_{18:1}C_{20:4}$			
72:4	$C_{18:1}C_{18:1}C_{18:1}C_{18:1}$	$C_{18:0}C_{18:1}C_{18:1}C_{18:2}$	$C_{18:0}C_{18:0}C_{18:2}C_{18:2}$		
		$C_{16:0}C_{16:0}C_{18:2}C_{22:2}$			
		$C_{16:0}C_{18:0}C_{18:0}C_{20:4}$			
72:3	$C_{18:0}C_{18:1}C_{18:1}C_{18:1}$				
72:2	$C_{18:0}C_{18:0}C_{18:1}C_{18:1}$	$C_{18:0}C_{18:0}C_{18:0}C_{18:2}$			
74:11			$C_{16:1}C_{16:1}C_{20:4}C_{22:5}$	$C_{16:1}C_{18:2}C_{18:2}C_{22:6}$	
			$C_{16:1}C_{16:1}C_{20:3}C_{22:6}$	$C_{16:1}C_{18:2}C_{20:4}C_{20:4}$	
			$C_{14:0}C_{16:1}C_{22:5}C_{22:5}$	$C_{14:0}C_{18:2}C_{20:4}C_{22:5}$	
			$C_{14:0}C_{20:4}C_{20:4}C_{20:3}$	$C_{14:0}C_{18:2}C_{20:3}C_{22:6}$	
			$C_{14:0}C_{18:1}C_{20:4}C_{22:6}$		
74:10			$C_{16:1}C_{18:1}C_{18:2}C_{22:6}$	$C_{16:1}C_{18:2}C_{20:4}C_{20:3}$	$C_{18:2}C_{18:2}C_{18:2}C_{20:4}$
			$C_{16:1}C_{18:1}C_{20:4}C_{20:4}$	$C_{16:0}C_{16:1}C_{20:3}C_{22:6}$	
			$C_{16:0}C_{16:0}C_{20:4}C_{22:6}$	$C_{16:0}C_{18:2}C_{18:2}C_{22:6}$	
				$C_{16:0}C_{18:2}C_{20:4}C_{20:4}$	
74:9		$C_{16:1}C_{18:1}C_{18:1}C_{22:6}$	$C_{16:1}C_{18:1}C_{20:4}C_{20:3}$	$C_{16:1}C_{18:2}C_{20:3}C_{20:3}$	$C_{18:2}C_{18:2}C_{18:2}C_{20:3}$
		$C_{18:1}C_{18:1}C_{18:1}C_{20:4}$	$C_{16:0}C_{18:1}C_{18:2}C_{22:6}$	$C_{18:1}C_{18:2}C_{18:2}C_{20:4}$	
			$C_{16:0}C_{18:1}C_{20:4}C_{20:4}$	$C_{16:0}C_{18:2}C_{20:4}C_{20:3}$	
			$C_{16:0}C_{16:0}C_{20:3}C_{22:6}$		
74:8			$C_{18:1}C_{18:1}C_{18:2}C_{20:4}$	$C_{16:1}C_{18:2}C_{20:2}C_{20:2}$	
74:7			$C_{16:1}C_{18:1}C_{20:3}C_{20:2}$	$C_{18:1}C_{18:2}C_{18:2}C_{20:2}$	
			$C_{16:1}C_{18:0}C_{20:4}C_{20:2}$	$C_{18:0}C_{18:2}C_{18:2}C_{20:3}$	
			$C_{16:1}C_{18:0}C_{20:3}C_{20:3}$		
			$C_{16:0}C_{18:2}C_{20:3}C_{20:2}$		
			$C_{16:0}C_{18:1}C_{20:4}C_{20:2}$		
			$C_{16:0}C_{18:1}C_{20:3}C_{20:3}$		
			$C_{16:0}C_{18:0}C_{20:4}C_{20:3}$		

			$C_{18:1}C_{18:1}C_{18:2}C_{20:3}$		
			$C_{18:0}C_{18:1}C_{18:2}C_{20:4}$		
74:6		$C_{16:0}C_{18:0}C_{18:0}C_{22:6}$	$C_{16:1}C_{18:1}C_{20:2}C_{20:2}$	$C_{16:0}C_{18:2}C_{20:2}C_{20:2}$	
		$C_{18:1}C_{18:1}C_{18:1}C_{20:3}$	$C_{16:1}C_{18:0}C_{20:3}C_{20:2}$	$C_{18:0}C_{18:2}C_{18:2}C_{20:2}$	
		$C_{18:0}C_{18:1}C_{18:1}C_{20:4}$	$C_{16:0}C_{18:1}C_{20:3}C_{20:2}$	$C_{18:0}C_{18:1}C_{18:2}C_{20:3}$	
			$C_{16:0}C_{18:0}C_{20:4}C_{20:2}$		
			$C_{16:0}C_{18:0}C_{20:3}C_{20:3}$		
			$C_{18:1}C_{18:1}C_{18:2}C_{20:2}$		
			$C_{18:0}C_{18:0}C_{18:2}C_{20:4}$		
74:5		$C_{18:0}C_{18:1}C_{18:1}C_{20:3}$	$C_{18:0}C_{18:0}C_{18:2}C_{20:3}$		
		$C_{18:0}C_{18:0}C_{18:1}C_{20:4}$			
74:4		$C_{18:0}C_{18:0}C_{18:1}C_{20:3}$			
		$C_{18:0}C_{18:0}C_{18:0}C_{20:4}$			
76:13			$C_{16:0}C_{16:1}C_{22:6}C_{22:6}$	$C_{16:1}C_{18:2}C_{20:4}C_{22:6}$	
				$C_{16:1}C_{20:4}C_{20:4}C_{20:4}$	
76:12			$C_{16:0}C_{16:0}C_{22:6}C_{22:6}$	$C_{16:0}C_{20:4}C_{20:4}C_{20:4}$	$C_{20:4}C_{20:3}C_{20:2}C_{16:2}$
			$C_{16:1}C_{18:1}C_{20:3}C_{22:6}$	$C_{16:1}C_{18:2}C_{20:2}C_{22:6}$	$C_{20:3}C_{20:3}C_{20:3}C_{16:2}$
76:11			$C_{16:1}C_{18:0}C_{20:4}C_{22:6}$	$C_{16:1}C_{20:4}C_{20:4}C_{20:2}$	$C_{18:2}C_{18:2}C_{20:4}C_{20:3}$
				$C_{16:1}C_{20:4}C_{20:3}C_{20:3}$	
				$C_{18:1}C_{20:2}C_{22:6}C_{16:2}$	
				$C_{18:0}C_{20:3}C_{22:6}C_{16:2}$	
				$C_{18:1}C_{18:2}C_{18:2}C_{22:6}$	
				$C_{18:1}C_{18:2}C_{20:4}C_{20:4}$	
76:10			$C_{16:1}C_{18:1}C_{20:2}C_{22:6}$	$C_{16:1}C_{20:4}C_{20:3}C_{20:2}$	$C_{20:4}C_{20:2}C_{20:2}C_{16:2}$
			$C_{16:1}C_{18:0}C_{20:3}C_{22:6}$	$C_{16:1}C_{20:3}C_{20:3}C_{20:3}$	$C_{20:3}C_{20:3}C_{20:2}C_{16:2}$
			$C_{18:0}C_{20:2}C_{22:6}C_{16:2}$	$C_{18:0}C_{18:2}C_{18:2}C_{22:6}$	$C_{18:2}C_{18:2}C_{20:4}C_{20:2}$
			$C_{18:1}C_{18:1}C_{18:2}C_{22:6}$	$C_{18:1}C_{18:2}C_{20:4}C_{20:3}$	$C_{18:2}C_{18:2}C_{20:3}C_{20:3}$
			$C_{18:1}C_{18:1}C_{20:4}C_{20:4}$	$C_{18:0}C_{18:2}C_{20:4}C_{20:4}$	
76:9		$C_{18:1}C_{18:1}C_{18:1}C_{22:6}$	$C_{16:0}C_{16:1}C_{22:4}C_{22:4}$	$C_{16:0}C_{18:2}C_{20:3}C_{22:4}$	
			$C_{16:1}C_{18:1}C_{20:3}C_{22:4}$	$C_{16:0}C_{20:3}C_{20:3}C_{20:3}$	
			$C_{16:0}C_{16:0}C_{22:5}C_{22:4}$	$C_{18:1}C_{18:2}C_{18:2}C_{22:4}$	
			$C_{16:0}C_{18:1}C_{20:4}C_{22:4}$	$C_{18:1}C_{18:2}C_{20:3}C_{20:3}$	
			$C_{16:0}C_{18:1}C_{20:3}C_{22:5}$		
			$C_{18:1}C_{18:1}C_{18:2}C_{22:5}$		
			$C_{18:1}C_{18:1}C_{20:4}C_{20:3}$		
76:8			$C_{18:1}C_{18:1}C_{20:3}C_{20:3}$	$C_{16:1}C_{20:2}C_{20:2}C_{20:2}$	
76:7			$C_{18:1}C_{18:2}C_{20:2}C_{20:2}$		
			$C_{18:1}C_{18:1}C_{20:3}C_{20:2}$		

Table 2: Ipsilateral/contralateral intensity ratios for various lipids species.

(a) Cortex-Contusional

Species	*m/z*	Average CCI ipsilateral/ contralateral	Std dev CCI ipsilateral/ contralateral	Average naïve ipsilateral/ contralateral	Std dev naïve ipsilateral/ contralateral	p-value Naïve vs CCI (red<0.05)
ST(d18:1/18:0)	806.55	1.644	0.648	1.021	0.046	0.370
PI(38:5)	883.53	0.446	0.134	1.135	0.020	0.011
PI(38:4)	885.55	0.361	0.122	1.014	0.168	0.030
ST(d18:1/24:1)	888.62	1.198	0.283	0.991	0.124	0.505
ST(d18:1/24:0)	890.64	1.892	0.878	1.016	0.155	0.358
ST(d18:1/h24:1)	904.62	1.182	0.254	1.012	0.017	0.516
CL(70:7)	1421.95	0.781	0.031	1.069	0.097	0.034
CL(70:6)	1423.96	0.809	0.045	1.025	0.056	0.035
CL(70:5)	1425.98	0.805	0.104	0.963	0.009	0.101
CL(70:4)	1428.00	0.772	0.058	1.023	0.067	0.041
CL(70:3)	1430.01	0.785	0.053	1.044	0.051	0.024
CL(72:9)	1445.95	0.760	0.045	1.041	0.128	0.073
CL(72:8)	1447.96	0.732	0.049	1.083	0.101	0.028
CL(72:7)	1449.98	0.596	0.078	1.105	0.149	0.031
CL(72:6)	1452.00	0.606	0.077	1.100	0.111	0.020
CL(72:5)	1454.01	0.590	0.094	1.098	0.083	0.017
CL(72:4)	1456.03	0.675	0.093	1.078	0.145	0.061
CL(72:3)	1458.04	0.822	0.044	1.115	0.118	0.057
CL(74:11)	1469.95	0.598	0.055	1.104	0.079	0.007
CL(74:10)	1471.96	0.516	0.090	1.085	0.086	0.012
CL(74:9)	1473.98	0.524	0.089	1.135	0.130	0.017
CL(74:8)	1476.00	0.456	0.120	1.110	0.103	0.016
CL(74:7)	1478.01	0.456	0.120	1.020	0.065	0.004
CL(74:6)	1480.03	0.540	0.100	1.050	0.130	0.031
CL(76:12)	1495.96	0.584	0.061	1.071	0.097	0.013
CL(76:11)	1497.98	0.503	0.064	1.082	0.089	0.007
CL(76:10)	1500.00	0.539	0.070	1.096	0.105	0.012
CL(76:9)	1502.01	0.651	0.090	1.072	0.055	0.019
CL(76:8)	1504.03	0.832	0.016	1.051	0.035	0.005
GM1(18:0)	1544.87	0.970	0.452	1.264	0.244	0.561
GM1(20:0)	1572.90	0.983	0.222	1.228	0.069	0.326
GD1(18:0)-H_2O	1817.95	1.022	0.564	1.301	0.211	0.639
GD1(20:0)-H_2O	1835.96	0.856	0.213	1.231	0.095	0.167

(b) **Cortex Non-contusional**

Species	*m/z*	Average CCI ipsilateral/ contralateral	Std dev CCI ipsilateral/ contralateral	Average naïve ipsilateral/ contralateral	Std dev naïve ipsilateral/ contralateral	p-value Naïve vs CCI (red<0.05)
ST(d18:1/18:0)	806.55	1.403	0.452	1.668	0.159	0.581
PI(38:5)	883.53	1.215	0.443	1.193	0.118	0.961
PI(38:4)	885.55	1.113	0.412	1.176	0.159	0.883
ST(d18:1/24:1)	888.62	1.164	0.506	1.574	0.046	0.442
ST(d18:1/24:0)	890.64	1.358	0.656	1.966	0.111	0.389
ST(d18:1/h24:1)	904.62	1.199	0.402	1.412	0.025	0.603
CL(70:7)	1421.95	1.015	0.027	1.010	0.002	0.879
CL(70:6)	1423.96	1.033	0.012	0.990	0.026	0.150
CL(70:5)	1425.98	1.042	0.004	1.036	0.096	0.940
CL(70:4)	1428.00	1.026	0.023	0.959	0.024	0.093
CL(70:3)	1430.01	1.042	0.007	0.988	0.007	0.008
CL(72:9)	1445.95	1.020	0.018	0.986	0.031	0.323
CL(72:8)	1447.96	1.185	0.117	1.030	0.012	0.244
CL(72:7)	1449.98	1.082	0.108	1.069	0.020	0.904
CL(72:6)	1452.00	1.085	0.085	1.043	0.031	0.637
CL(72:5)	1454.01	1.129	0.137	1.084	0.019	0.744
CL(72:4)	1456.03	1.076	0.074	1.050	0.015	0.728
CL(72:3)	1458.04	0.988	0.016	1.032	0.062	0.427
CL(74:11)	1469.95	1.029	0.096	1.034	0.005	0.953
CL(74:10)	1471.96	1.060	0.100	1.046	0.045	0.888
CL(74:9)	1473.98	1.062	0.111	1.060	0.016	0.982
CL(74:8)	1476.00	1.155	0.207	1.138	0.073	0.935
CL(74:7)	1478.01	1.155	0.207	1.127	0.061	0.861
CL(74:6)	1480.03	1.106	0.135	1.087	0.016	0.889
CL(76:12)	1495.96	1.033	0.050	1.001	0.011	0.546
CL(76:11)	1497.98	0.999	0.099	1.067	0.011	0.507
CL(76:10)	1500.00	1.039	0.064	1.034	0.022	0.932
CL(76:9)	1502.01	1.009	0.053	1.041	0.006	0.555
CL(76:8)	1504.03	0.983	0.028	0.996	0.031	0.733
GM1(18:0)	1544.87	1.505	0.572	1.375	0.301	0.834
GM1(20:0)	1572.90	1.382	0.265	1.328	0.429	0.901
GD1(18:0)-H_2O	1817.95	1.550	0.606	1.467	0.251	0.896
GD1(20:0)-H_2O	1835.96	1.131	0.115	1.133	0.136	0.990

(c) **Hippocampus**

Species	*m/z*	Average CCI ipsilateral/ contralateral	Std dev CCI ipsilateral/ contralateral	Average naïve ipsilateral/ contralateral	Std dev naïve ipsilateral/ contralateral	p-value Naïve vs CCI (red<0.05)
ST(d18:1/18:0)	806.55	1.203	0.230	1.051	0.153	0.568
PI(38:5)	883.53	0.830	0.081	1.054	0.064	0.085
PI(38:4)	885.55	0.725	0.090	0.963	0.128	0.157
ST(d18:1/24:1)	888.62	0.936	0.115	1.014	0.143	0.641
ST(d18:1/24:0)	890.64	1.261	0.363	1.109	0.269	0.722
ST(d18:1/h24:1)	904.62	1.020	0.098	1.034	0.115	0.919
CL(70:7)	1421.95	0.884	0.035	0.997	0.022	0.053
CL(70:6)	1423.96	0.882	0.029	0.991	0.032	0.055
CL(70:5)	1425.98	0.864	0.033	1.006	0.021	0.007
CL(70:4)	1428.00	0.862	0.032	1.000	0.039	0.045
CL(70:3)	1430.01	0.861	0.029	1.013	0.014	0.013
CL(72:9)	1445.95	0.910	0.029	1.005	0.022	0.055
CL(72:8)	1447.96	0.890	0.051	1.057	0.016	0.041
CL(72:7)	1449.98	0.755	0.043	1.035	0.015	0.006
CL(72:6)	1452.00	0.772	0.049	1.007	0.003	0.014
CL(72:5)	1454.01	0.765	0.025	1.039	0.013	0.002
CL(72:4)	1456.03	0.794	0.019	1.008	0.014	0.002
CL(72:3)	1458.04	0.874	0.017	0.994	0.008	0.006
CL(74:11)	1469.95	0.797	0.033	0.995	0.025	0.011
CL(74:10)	1471.96	0.709	0.041	0.998	0.000	0.004
CL(74:9)	1473.98	0.695	0.054	1.025	0.005	0.007
CL(74:8)	1476.00	0.650	0.043	1.048	0.038	0.004
CL(74:7)	1478.01	0.650	0.043	1.037	0.038	0.001
CL(74:6)	1480.03	0.717	0.034	1.022	0.015	0.003
CL(76:12)	1495.96	0.784	0.023	1.008	0.008	0.002
CL(76:11)	1497.98	0.684	0.030	1.009	0.013	0.002
CL(76:10)	1500.00	0.707	0.041	1.031	0.003	0.003
CL(76:9)	1502.01	0.749	0.033	1.010	0.004	0.003
CL(76:8)	1504.03	0.862	0.015	0.979	0.022	0.012
GM1(18:0)	1544.87	0.991	0.102	1.134	0.037	0.239
GM1(20:0)	1572.90	1.030	0.106	1.216	0.071	0.190
GD1(18:0)-H_2O	1817.95	0.976	0.114	1.153	0.048	0.206
GD1(20:0)-H_2O	1835.96	0.968	0.068	1.086	0.026	0.167

(d) Thalamus						
Species	***m/z***	**Average CCI ipsilateral/ contralateral**	**Std dev CCI ipsilateral/ contralateral**	**Average naïve ipsilateral/ contralateral**	**Std dev naïve ipsilateral/ contralateral**	**p-value Naïve vs CCI (red<0.05)**
ST(d18:1/18:0)	806.55	1.139	0.267	1.052	0.095	0.754
PI(38:5)	883.53	0.913	0.054	1.031	0.089	0.252
PI(38:4)	885.55	0.853	0.028	0.982	0.006	0.015
ST(d18:1/24:1)	888.62	1.019	0.335	1.032	0.217	0.971
ST(d18:1/24:0)	890.64	1.124	0.393	1.059	0.186	0.877
ST(d18:1/h24:1)	904.62	1.100	0.242	1.035	0.126	0.804
CL(70:7)	1421.95	0.955	0.075	0.998	0.019	0.584
CL(70:6)	1423.96	0.902	0.036	0.996	0.011	0.070
CL(70:5)	1425.98	0.892	0.058	0.994	0.010	0.070
CL(70:4)	1428.00	0.909	0.036	0.991	0.003	0.092
CL(70:3)	1430.01	0.886	0.037	0.985	0.030	0.094
CL(72:9)	1445.95	0.906	0.029	0.990	0.003	0.053
CL(72:8)	1447.96	0.855	0.054	1.020	0.024	0.051
CL(72:7)	1449.98	0.849	0.041	0.998	0.024	0.036
CL(72:6)	1452.00	0.829	0.004	0.980	0.009	0.000
CL(72:5)	1454.01	0.851	0.019	1.006	0.008	0.004
CL(72:4)	1456.03	0.866	0.016	0.980	0.016	0.008
CL(72:3)	1458.04	0.946	0.064	0.987	0.016	0.544
CL(74:11)	1469.95	0.753	0.065	0.984	0.004	0.030
CL(74:10)	1471.96	0.774	0.022	0.979	0.025	0.005
CL(74:9)	1473.98	0.740	0.025	0.976	0.004	0.002
CL(74:8)	1476.00	0.799	0.069	0.981	0.006	0.065
CL(74:7)	1478.01	0.799	0.069	1.021	0.065	0.030
CL(74:6)	1480.03	0.879	0.096	0.995	0.006	0.276
CL(76:12)	1495.96	0.749	0.070	0.959	0.042	0.060
CL(76:11)	1497.98	0.701	0.040	0.955	0.027	0.009
CL(76:10)	1500.00	0.718	0.053	0.973	0.014	0.014
CL(76:9)	1502.01	0.802	0.005	0.983	0.006	0.000
CL(76:8)	1504.03	0.897	0.041	0.979	0.010	0.119
GM1(18:0)	1544.87	0.988	0.089	1.111	0.148	0.438
GM1(20:0)	1572.90	0.863	0.137	1.082	0.042	0.188
GD1(18:0)-H_2O	1817.95	1.005	0.113	1.105	0.147	0.550
GD1(20:0)-H_2O	1835.96	0.958	0.066	1.056	0.089	0.352

Table 2: Ipsilateral/contralateral intensity ratios for various lipids species including CL's, PI, sulfatides and gangliosides were assessed for the following areas noted in the optical image in Figures 1 and 2: the contusional area (a), a cortical area adjacent to the contusional area (b), the hippocampus (c) and the thalamus (d).

Supporting Method 1: Spectra Acquisition and Data Conversion for .t2d Files on the ABI-4800 MALDI for Tissue Imaging with full random walking

Summary: This system allows MALDI-MS imaging using full random walk capabilities[1] on an ABI 4800 instrument. Spectra are acquired with just the ABI 4000-series control software using a custom geometry setting and converted into an imzML data cube file using open source software. This data cube file can then be analyzed to generate MALDI images for various *m/z* values. This assumes that tissue sections have already been prepared on conductive ITO slides. This protocol requires an AB 4800 Slide Glass Guide for 2 pieces (Hudson Surface Technology, Old Tappan, NJ) to fit the ITO tissue slides onto an ABI metal base plate. The data conversion has been performed on a computer running Microsoft Windows 7 Enterprise 64-bit (www.windows.com) with Oracle Java runtime environment installed (www.java.com).

OUTLINE:

I. Spectra Acquisition on the ABI-4800 MALDI for Tissue Imaging
   a. Mark the four corners of a rectangular imaging area around the tissue slice
   b. Estimate the coordinates of the 4 corner spots
   c. Setup & load a custom plate geometry based on these coordinates
   d. Insert sample and start batch run to generate an array of t2d spectra files

II. Data Conversion for .t2d Files
   a. Conversion of each .t2d file into an .mzXML file.
   b. All .mzXML files will be converted into an .mzML files (converter compatibility).
   c. All .mzML files will be combined into a single .imzML file.
   d. This image file can then be opened in an imzML viewer like Datacube Explorer or MSiReader.

[1] This very involved method was developed so that full-random walk imaging could be performed on the ABI-4800 MALDI instrument using open source software. Full random-walking within each pixel location was necessary in order to detect very low abundance brain cardiolipin. Higher-abundance lipids could be detected without random walking, and there are other open source tools that can perform imaging without random walking, such as 4000 Series Imaging by Markus Stoeckli (available at http://maldi-msi.org).

I. Spectra Acquisition on the ABI-4800 MALDI for Tissue Imaging

Goal: Performing an imaging run with random walking on an ABI-4800 MALDI-TOF/TOF using the bundled 4000 instrument control software.

The process is split into four steps:

1. Mark the four corners of a rectangular imaging area around the tissue slice
2. Estimate the coordinates of the 4 corner spots
3. Setup & load a custom plate geometry based on these coordinates
4. Insert sample and start batch run to generate an array of t2d spectra files

1. Select the area to be imaged and mark the corners

In theory any shape can be imaged on the ABI-4800 instrument, but a software limitation in one of the file converters limits this to a rectangular shape. More advanced shapes could be defined within a rectangle if the unused imaging locations are removed from the batch run prior to generating the imzML file (see Data Conversion section).

a. Four reference marks are drawn on the ITO slide around the tissue sections as in any other MALDI imaging experiment. Since the illumination inside the MALDI source varies, it might require a dark sharpie, silver sharpie, or a white-out pen in order to best see these marks with the video viewer (see page 2-12 of the Applied Biosystems/MDS SCIEX 4800 MALDI TOF/TOF™ Analyzer Hardware Guide for adjusting the video viewer). If these marks are made on the back side of the ITO slide, then the alignment will be slightly off but the marker will not accidentally contaminate the tissue.

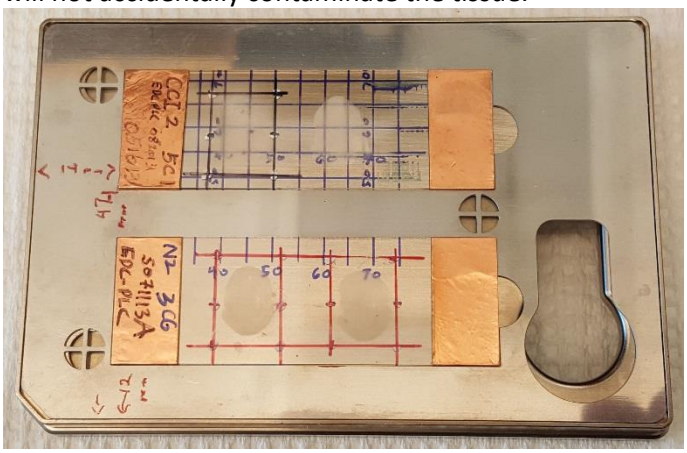

Figure 1: Base metal plate with adapter sheets and ITO slides. Marked area for the imaging is in red ink with the reference marks at the four corners of the rectangles around the tissue section.

b. The experimental slide is put into the upper slot on the plate adapter and a calibration/test slide in the lower slot.[2]

[2] For convenience it is best to put the experimental slide in the top slot and to orient the slides so that the bottom of the slide (with our notations about the tissue section) is always next to the left side of the slide adapter. If the

2. Get the coordinates of the four corners of the imaging area

Drawing grid with x and y coordinates on the metal base plate will help make the next steps easier. The coordinate system that the instrument control software uses starts in the notched bottom left corner. The instrument's coordinates are in µm. An estimate of the upper-left corner of the imaging area is needed around the tissue on the experimental side. By the way the numbers run, this is the x-minimum and y-maximum for the imaging area, see Figure 3 for an example.

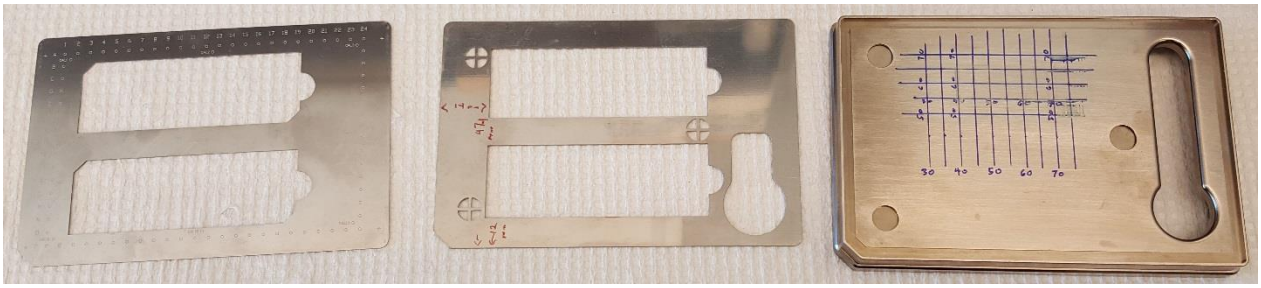

Figure 2: (left and middle) A set of slide adapter sheets, (Hudson Surface Technology, Old Tappan, NJ); (right) ABI base plate.

a. Load the plate as any spot set, load any acquisition & analysis method and switch to manual control of the stage.
b. Using the video viewer, find the upper-left reference mark that was made so that it is under the crosshairs of the optical camera. If the coordinate values above have been estimated, then they can be manually entered and the joystick can be used for fine adjustment. Make sure the lamp is set for best contrast so that the marks can be seen clearly (page 2-12, ABI-4800 Hardware Guide).
c. Using the joystick and (x,y) readout, move horizontally and vertically to find the other corners and make a note of the exact (x,y). Since the lateral resolution we desire in this present work is 200 microns, round these up to the nearest 200 microns. In this example it is x=58000 and y =70000.

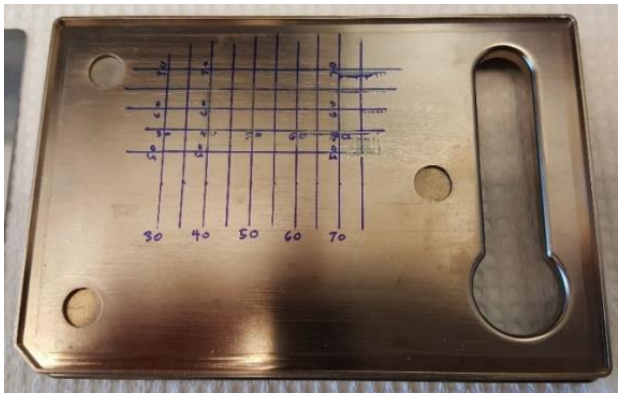

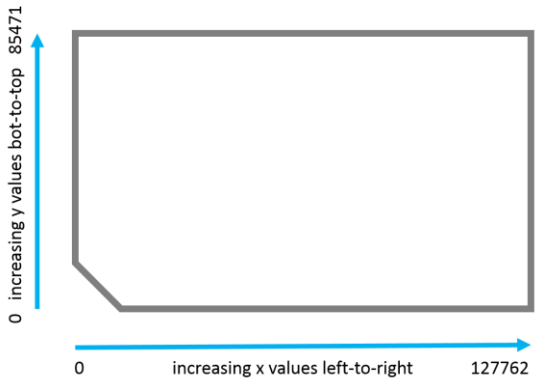

tissue sections always go on the same general location on the ITO slides, this makes estimating the x,y coordinates and generating a spot set much easier.

Figure 3: (Left) ABI base metal plate with coordinate system drawn on it for reference with a t-square and millimeter ruler -- the x and y coordinates (Right) start in the bottom left corner.

3. Create the custom plate geometry for the control software

Each imaging location or "pixel" in the imaging run needs a coordinate so the instrument can perform the random walking within this pixel (section 3-4, ABI Getting Started Guide to the 4800). The plate geometry file defines for the instrument where the pixels are. Since the tissue locations are never going to be exactly the same size or location on the slides, each ITO slide requires a custom plate geometry and spot set. In this step a very fine grid is being created, similar to the well coordinate system on the metal plates that are commonly used on top of the metal base plates with the instrument. In this case, we are making a rectangular grid of pixels, each of which are 200 microns in size. The structure of the xml file can be seen in this example below (Template_TOP_200u.txt), where the grid for one area is defined. As mentioned earlier the instrument uses µm as their unit of measurement[3]. For convenience the spots on the top row are labeled from "AA01" to "AA99", going left to right (increasing x coordinates). The next row down (decreasing y coordinates) is "AB01" to "AB99" and so on. Continuing this to the "DU" row gives a 99x99 grid of spots, each 200x200 microns in size. This covers an area of 19.8mm x 19.8mm, which is more than enough to cover the brain sections that this method has been used for

Template_TOP_200u.txt

```
<TsquaredData modifiedDT="04/23/2016 15:26:32">
<PlateType name="TOP_SECTION" description="Plate name" width="127762"
height="85471">

INSERT SPOT SET HERE (see example structure below in green)

<Spot label="AA01" shape="E" width="200" height="200" x="58000" y="70000"/>
..
<Spot label="AA99" shape="E" width="200" height="200" x="77600" y="70000"/>
<Spot label="AB01" shape="E" width="200" height="200" x="58000" y="69800"/>
..
<Spot label="AB99" shape="E" width="200" height="200" x="77600" y="69800"/>
..
<Spot label="DU98" shape="E" width="200" height="200" x="77400" y="50000"/>
<Spot label="DU99" shape="E" width="200" height="200" x="77600" y="50000"/>

</PlateType>
<SpotSetTemplate name="TOP_SECTION" description="Plate name"
plateType="TWO_SECTION">

INSERT SPOT SET HERE ALSO

</SpotSetTemplate>
</TsquaredData>
```

The first imaging location should have the x and y coordinates of the upper left corner of the imaging area (in this example it is x=58000 and y =70000). Spots AA1 to AA99 define the first row, moving incrementally from row AB to AC to finally DU the whole are of the grid is defined. This file can also be setup two contain two non-adjacent areas to be imaged, starting the second area with a spot label such

[3] Example files of everything mentioned here, such as the auto-filling spreadsheet, are available from the authors

as “MA01”, for example. The advantage of two areas is the option to queue both areas in batch mode and perform the runs sequentially.

As typing in thousands of coordinates would be time consuming, the spot set coordinate grid for this file was created using a spreadsheet program (such as Microsoft Excel). A small PowerShell script could be used instead of a spreadsheet. A short summary of the Excel spreadsheet is below.

a. Open a new spreadsheet file and separate the first spot label row from the Template_TOP_200u.txt file into multiple columns:

	A	B	C	D	E	F	G	H
1	<Spot label="	AA	01	" shape="E" width="200" height="200" x="	58000	" y="	70000	"/>
2	<Spot label="	AA	02	" shape="E" width="200" height="200" x="	=E01 +200	" y="	70000	"/>
2	<Spot label="	AA	03	" shape="E" width="200" height="200" x="	=E02 +200	" y="	70000	"/>

b. In cell E1 type in the upper-left x coordinate (in microns), and in G1 the upper-left y coordinate (in microns). If the spreadsheet is set up properly the other rows will auto-fill.
c. Any x-values spots that are above the x-maximum (i.e. to the right of the desired imaged area) can be removed with the filter command in Excel (found at Data->Filter->AutoFilter) and y values below y-minimum (i.e. below the imaging area) can be removed by just deleting the last several rows.
d. Copy all cells that contain visible values. The Excel file is no longer needed at this point, although saving it will make it easier to set up future imaging runs.
e. Use Notepad (or a different text editor) to open the new plate type and spot list file “Template_TOP_200u.txt” and paste these spot values into both of the two locations noted. Excel automatically adds tabs to mark columns. To remove these, use the replace-all command in Notepad to replace all of the tabs with empty spaces.
f. Choose a descriptive name for the plate type, and add this name to the two locations noted[4]. Choose a name for the spot set, and add that to the location noted.
g. Save this as "all file types" on the drop-down menu and with a .XML extension.
h. In the 4000 Control software, select File->XML Database Import. Import the XML file that was just created in the previous step. (this could take around 15 minutes depending on the number of spots and the instrument computer’s speed -- and this is why the HV was turned on several steps ago to give it a chance to warm up)
i. Select File->New->New Spot Set. Pick names for the plate and spot set[5]. For the Spot Set template, go to the User-defined directory, and the spot set that was created previously should be there.

4. Insert the sample and start the batch run.

[4] For this present work it was "slide name_(TOP/BOT)_200u", indicating the source of the source of the tissue slice, whether it is the top or bottom section, and the lateral resolution (200 microns).
[5] It is easier to keep things consistent and use the same name chosen previously few steps ago.

Obviously, all the instrument methods (acquisition and analysis) should be thoroughly tested before starting the actual imaging run (number of shoots, power, fragmentation window and settings & standards). Performing imaging as a batch-run of a series of spectral acquisitions allows any instrument method to be used for imaging, especially those with random walking.

a. Eject the plate. Re-insert it, but using the spot set that was just defined. Give the vacuum and HV some time to stabilize. Give the laser a few test shots away from the imaging location (a second tissue slide can be loaded on the slide adapted, prepared identically, to test the laser). Go to the upper left corner of the imaging area to check the alignment. Since the video viewer is not needed during the run, turn the lamp down to 0 (saves the bulb, and saves the tissue from being exposed to light during a long imaging run)
b. Hit the button to select Batch mode. Select all lines in the spot set, then right click and Copy Spots to Job->Using Latest Methods
c. In the Acquisition and processing columns, select the methods that were previously opened/prepared.
d. File->Validate Spot Set to check for errors
e. Batch->Submit Spot Set Job
f. Batch->Start Spot Set Job
g. When the run is over, Batch->Stop Job Queue. Click the button to leave Batch mode. Select all lines in the batch run, then Copy Selected Items to a disk location to save the imaging run as a set of spectra files in T2D format.

II. Data Conversion for .t2d Files

Goal: Convert spectra acquired from a custom geometry plate on the ABI 4800 into an imzML data cube file (Strum et al, 2012), which can then be analyzed to generate images for various *m/z* values

Starting situation: Folder contains .t2d spectra of every pixel as a single file. As of now only rectangular geometries can be converted (imzMLConverter limitation).

The conversion itself is done in four steps:

1. Conversion of each .t2d file into an .mzXML file.
2. All .mzXML files will be converted into an .mzML files (for imzML converter compatibility).
3. All .mzML files will be combined into a single .imzML file.
4. This image file can then be opened in an imzML viewer like Datacube Explorer or MSiReader.

1) Download, install and run the T2D Conveter.

a) Written by Yu (Tom) Gao (www.pepchem.org) and uses OpenMS tools (Strum et al., 2008).
b) Download from http://www.pepchem.org/download/converter.html
c) Start the program, point it to the directory with the .t2d files.

d) The converted files (.mzxml) will be generated in the same folder.
e) Requires the current java runtime routine to be installed (www.java.com).

2) Download, install and run ProteoWizard (Chambers et al., 2012).

a) http://proteowizard.sourceforge.net/
b) Use Windows PowerShell to convert the files via msconvert from ProteoWizard.
   i) Start Windows PowerShell or the command line (cmd)[6].
   ii) Switch into the ProteoWizard directory in PowerShell or the command line (cmd) by typing this command: cd 'C:\Program Files (x86)\ProteoWizard\ProteoWizard 3.0.7331'
   iii) If ProteoWizard is in a different directory (and newer version probably will be) then that current correct directory name will need to be used[7].
c) Use ProteoWizard to convert from .mzxml to .mzml by typing this command:

msconvert 'C:\your data directory *.mzxml' -o 'C:\your data directory' –v

3) Download, install and run imzMLConverter (Race et al., 2012).

a) http://www.cs.bham.ac.uk/~ibs/imzMLConverter/
b) In the Input Files tab, select the appropriate files, set the size of the image via the number of pixels in x and y direction, select one spectrum per file.
c) Sometimes this program doesn't find the files on the first try – if that happens try adding the files again
d) In the Image tab, in data file content, select "MS1 spectrum"
e) Hit "convert" and select file name for the resulting imzML datacube.

4) Download, install and run MSiReader (Robichaud et al., 2013)[8].

a) http://www4.ncsu.edu/~dcmuddim/msireader.html
   i) Also install the necessary Matlab runtime environment (see MSiReader documentation).
b) Open the final .imzML file with MSiReader.

General comments: Conversion should be done on a fast Windows machine; a solid state hard drive will considerably speed up the conversion. The above mentioned method does not require the original .t2d viewer from the manufacturer on that computer. A current java runtime routine needs to be installed.

Scripting: The paths for the windows installation should be adapted/updated accordingly, the same applies for the location of the data files and paths for msconvert. Windows PowerShell is a capable option to run scripts under windows, using its auto completion feature helps to fill out the file paths under Windows. It is a superior alternative to the Windows command prompt (cmd).

---

[6] Windows PowerShell can be started by left-clicking on the Start Menu at the bottom-left of the desktop and typing "PowerShell" into the search box. There are several general guides for using PowerShell available online, although all that is needed to follow these directions are the two commands given above.
[7] Expert PowerShell users can save time by temporarily adding Msconvert to the path variable:
$env:Path += ";C:\Program Files (x86)\ProteoWizard\Proteowizard 3.0.7331"
[8] Alternatively, Datacube Explorer could be used to analyze the data:
http://www.amolf.nl/download/datacubeexplorer/

References for Supporting Method 1:

Chambers,M.C., MacLean,B., Burke,R., Amode,D., Ruderman,D.L., Neumann,S., Gatto,L., Fischer B., Pratt B., Egertson J., Hoff K., Kessner D., Tasman N., Shulman N., Frewen B., Baker T.A., Brusniak M.-Y., Paulse C., Creasy D., Flashner L., Kani K., Moulding C., Seymour S.L., Nuwaysir L.M., Lefebvre B., Kuhlmann F., Roark J., Rainer P., Detlev S., Hemenway T., Huhmer A., Langridge J., Connolly B., Chadick T., Holly K., Eckels J., Deutsch E.W., Moritz R.L., Katz J.E., Agus D.B., MacCoss M., Tabb D.L. & Mallick P. (2012) A cross-platform toolkit for mass spectrometry and proteomics. Nat. Biotech. 30, 918-920.

Race A. M., Styles I. B., Bunch J. (2012) Inclusive sharing of mass spectrometry imaging data requires a converter for all. J. Proteomics, 75, 5111-5112.

Robichaud G., Garrard K. P., Barry J. A., Muddiman D. C. (2013) MSiReader: An Open-Source Interface to View and Analyze High Resolving Power MS Imaging Files on Matlab Platform. J. Am. Soc. Mass. Spectrom., 24, 718-721. DOI: 10.1007/s13361-013-0607-z.

Schramm T, Hester A, Klinkert I, Both J-P, Heeren RMA, Brunelle A, Laprévote O, Desbenoit N, Robbe M-F, Stoeckli M, Spengler B, Römpp A (2012) imzML — A common data format for the flexible exchange and processing of mass spectrometry imaging data. Journal of Proteomics 75 (16):5106-5110. doi:10.1016/j.jprot.2012.07.026

Sturm M., Bertsch A., Gröpl C., Hildebrandt A., Hussong R., Lange E., Pfeifer N., Schulz-Trieglaff O., Zerck A., Reinert K., and Kohlbacher O. (2008) OpenMS – an Open-Source Software Framework for Mass Spectrometry. BMC Bioinformatics 9, 163. doi:10.1186/1471-2105-9-163.